International Journal of Computer Information Systems and Industrial Management Applications
ISSN 2150-7988 Volume 18(4s) 2026 pp. 1325-1345
https://doi.org/10.70917/ijcisim-2026-2639
Article

DEVELOPMENT OF A VALIDATED DIGITAL TWIN MODEL FOR POWER-SPLIT HYBRID ELECTRIC VEHICLE DYNAMICS

Pradeep Gaikwad[1], Ramdas G. Biradar[2]

[1,2]School of Engineering and Technology, Pimpri Chinchwad University, Pune, India
*Corresponding author: pradeep.gaikwad23@pcu.edu.in

Abstract:A physics-based digital twin model of a power-split hybrid electric vehicle is developed to reproduce the coupled behaviour of the internal combustion engine, motor-generator units, high-voltage battery, DC-DC converter, planetary gear power-split device and longitudinal vehicle body. The model is formulated in a modular MATLAB/Simulink and Simscape environment so that each subsystem can be parameterized, monitored and validated without losing the energy interactions that govern hybrid powertrain operation. The vehicle model uses a 1575 kg vehicle mass, 0.30 m tyre radius, 75 kW engine, 25 kW MG1, 55 kW MG2, 650 V regulated DC bus and 70% initial battery state of charge. A rule-based supervisory energy management strategy is integrated with explicit mode-selection, torque-split, SOC-protection and regenerative-braking logic. Validation is carried out using a reference-response drive-cycle procedure and quantitative error metrics. The developed model tracks the 0-100 km/h speed profile with a speed RMSE of 0.76 km/h, speed MAE of 0.59 km/h and speed MAPE of 3.08%. The high-voltage battery remains within 69.61-70.25% SOC, while the battery voltage is maintained between 339 and 341 V and the DC-link voltage remains close to 650 V with a DC-link RMSE of 1.38 V. The results demonstrate stable power sharing between engine, MG1, MG2 and battery, with battery power varying from approximately -20 kW during charging/regeneration to +40 kW during traction assistance. The proposed digital twin provides a transparent and computationally practical platform for HEV performance evaluation, power-flow analysis, controller verification and future health-monitoring applications.

Keywords: Digital twin; power-split hybrid electric vehicle; MATLAB/Simulink; energy management; battery SOC; planetary gear; DC-DC converter; validation metrics

1. Introduction

Hybrid electric vehicles are a practical transition technology for reducing fuel consumption and tail-pipe emissions while maintaining the driving range and refuelling convenience of conventional powertrains [1]. Among the available hybrid configurations, the power-split architecture has gained considerable importance because it combines the advantages of series and parallel hybrid operation through a planetary gear set. In this arrangement, the internal combustion engine, generator and traction motor interact continuously, and the demanded wheel power can be supplied by engine power, battery power or a combination of both [2]. This flexibility improves fuel economy, but it also makes the dynamic response of the complete vehicle difficult to analyse using isolated subsystem models. The digital twin concept provides a suitable framework for such a coupled vehicle system because it represents the physical asset through a synchronized virtual model that can reproduce system states, calculate hidden variables and support predictive decisions [3]. In an automotive powertrain, the digital twin is not only a graphical simulation. It must contain a physics-based plant model, measured or reference inputs, controller logic, validation metrics, calibration feedback and analytics capable of explaining the power flow between mechanical and electrical domains [4]. The model becomes useful only when it can quantify the deviation between the virtual response and a reference response using numerical error indices.

A power-split HEV is especially suitable for digital twin development because its performance depends on interactions among the engine, the generator, the traction motor, the high-voltage battery, the power electronics and the vehicle body [5]. For example, an acceleration demand increases the tractive power required at the wheels, which changes MG2 torque, engine torque, battery current and DC-link power. During regenerative braking, the direction of power flow reverses and the battery receives charging current subject to SOC and voltage limits. A reliable digital twin must therefore model torque distribution, speed coupling, battery charge variation, converter regulation and longitudinal vehicle motion in a common simulation environment [6]. The present work develops a validation-oriented digital twin model for a power-split HEV using MATLAB/Simulink and Simscape. The model includes an internal combustion engine, MG1, MG2, lithium-ion battery, DC-DC converter, planetary gear based power-split device and longitudinal vehicle body. In addition to the conventional modelling of components, the study introduces an explicit digital twin architecture, mathematical formulation, control logic, parameter-source justification and quantitative validation using RMSE, MAE, MAPE and percentage error. These additions are important because many existing simulation studies present only waveform outputs without demonstrating accuracy, repeatability and model reliability [7]. The main contribution of this study is an integrated digital twin framework that links component-level equations and system-level control decisions for a power-split HEV. The model is designed to reproduce acceleration, braking, electric assist, engine driving, battery charge-discharge and DC-link regulation over a reference driving cycle. The work further provides a benchmark comparison and detailed interpretation of results, including battery power limits, SOC envelope, speed tracking, converter stability, braking response and power-flow transitions [8]. The structure is scalable for future inclusion of real vehicle sensor data, onboard diagnostics and predictive maintenance algorithms.

2. LITERATURE REVIEW

The literature related to the present work can be grouped into three streams: digital twin technology for electric and hybrid vehicles, energy management of power-split hybrid powertrains and validation methods for model-based vehicle simulation. Digital twin studies emphasize real-time monitoring, predictive analysis and cyber-physical synchronization. Power-split HEV studies emphasize planetary gear modelling, engine-motor coordination and optimal energy distribution. Validation studies emphasize the need to compare model outputs against reference cycles, benchmark models or experimental measurements [9]. A useful HEV digital twin must combine these three streams rather than treating them separately. Digital twin technology has been widely discussed for electric vehicle powertrains and battery systems because it can support diagnostics, state estimation, predictive maintenance and virtual testing [10]. Reviews of EV powertrain digital twins highlight the importance of combining sensing, physics-based modelling and data-driven correction layers. Battery-focused studies further indicate that digital twins can improve SOC, SOH and remaining useful life estimation when the virtual model is continuously updated using measured data [11]. However, a battery-only twin cannot explain the complete behaviour of a power-split HEV because engine torque, motor torque, gear kinematics and vehicle load strongly influence the battery current and SOC trajectory.

Energy management of power-split HEVs has been studied using rule-based control, model predictive control, dynamic programming, equivalent consumption minimization, fuzzy logic and reinforcement learning [12]. Predictive and learning-based strategies can improve fuel economy, but they usually require a reliable plant model and validated component parameters. Rule-based control remains relevant for digital twin development because its transparent decisions allow easy verification of mode transitions and power-flow direction. In the present work, a rule-based supervisory strategy is selected because the primary objective is to establish a validated plant-controller digital twin that can later be extended to MPC or learning-based control [13]. The literature also shows that simulation-only studies become weak when they do not include validation or quantitative error values. For journal-level HEV modelling, validation may be carried out against experimental vehicle data, chassis-dynamometer data, standard driving-cycle references, published benchmark responses or a validated high-fidelity model [14]. This study applies a reference-response validation protocol suitable for the available Simulink model and reports speed, SOC and DC-link voltage error metrics. The approach provides a practical foundation for later experimental validation with CAN bus signals or dynamometer measurements [15].

Table 2. Literature synthesis used to develop the proposed HEV digital twin framework

Study	Focus area	Major contribution	Gap connected with this paper
Li et al. [4]	Digital twin for EV powertrain	Reviewed EV powertrain twin architecture, applications and challenges.	Need for complete powertrain-level twin with validation.
Saba et al. [16]	Battery digital twins	Showed value of digital twins in battery analysis and intelligent transportation.	Battery twin must be connected to vehicle power demand and converter response.
Ye et al. [17]	Digital twin with learning control	Used a digital twin approach to enhance learning-based energy management.	HEV power-split dynamics require transparent plant equations before learning control.

Study	Focus area	Major contribution	Gap connected with this paper
Castellano et al.[18]	MPC for power-split HEV	Presented model predictive control for multimode power-split hybrid transmission.	Plant models need validation and practical implementation structure.
Chen et al. [19]	Stochastic MPC and reinforcement learning	Integrated predictive control and learning for power-split plug-in HEV energy management.	Model-based control depends on accurate SOC and power-flow representation.
Dong et al.[20]	Explicit MPC for dual-mode power-split HEV	Improved real-time feasibility of optimal energy management.	Digital twin analytics layer is needed for continuous model assessment.
Borhan et al. [21]	Nonlinear MPC for power-split HEV	Applied predictive control to nonlinear energy management.	Controller equations should be linked with vehicle-level dynamics.
Li et al. [22]	Single planetary gear design	Explained systematic design of split hybrid vehicles using a planetary gear.	Kinematic and torque coupling of planetary gear must be included in digital twin.
MathWorks [23]	Power-split HEV reference model	Provides reference architecture for power-split hybrid vehicle electrical network.	Reference model should be customized, interpreted and validated for research use.
Polat [24]	Digital twin for light electric vehicle	Compared motor performance using digital twin and road input data.	HEV digital twin additionally needs engine-generator and planetary gear layers.
Liu et al.[25]	Power-split driveline vibration	Studied active damping of power-split hybrid drivetrain vibration.	Dynamic torque transients should be considered in future twin refinement.
Li et al. [26]	EV powertrain system based on digital twin	Presented digital-twin-based simulation testing framework.	Power-split HEV requires integrated mechanical and electrical coupling.

1.1 Novel Contribution and Research Gap

The research gap addressed in this paper is the absence of an integrated and quantitatively validated digital twin model for the complete dynamics of a power-split HEV. Recent digital twin studies often focus on electric vehicle batteries, charging systems or generic EV powertrains, whereas power-split HEV research commonly concentrates on energy management without establishing a complete cyber-physical model [27]. A digital twin intended for HEV dynamics must combine the vehicle plant, energy management controller, standard input cycle, reference comparison and numerical error evaluation in one consistent framework. The proposed model contributes to this gap in four ways [28]. First, the vehicle is represented as a coupled mechanical-electrical-control system rather than as separate subsystem plots. Second, the planetary gear power-split relation, battery SOC dynamics, DC-DC converter behaviour and longitudinal vehicle equations are documented mathematically [29]. Third, the supervisory controller is expressed through transparent rules for electric drive, engine drive, hybrid assist and regenerative braking. Fourth, the model is assessed using quantitative validation metrics and benchmark comparison instead of relying only on visual agreement of simulation signals [30].

Table 3. Main novelty of the proposed model in comparison with common HEV simulation approaches

Aspect	Common limitation in previous studies	Approach adopted in this study
Model scope	Subsystem-level battery, motor or energy management models are often reported separately.	Engine, MG1, MG2, battery, DC-DC converter, power-split device and vehicle body are integrated in one model.

Aspect	Common limitation in previous studies	Approach adopted in this study
Digital twin definition	Simulation is sometimes described as a digital twin without data, feedback or validation layer.	The architecture includes physical layer, data/input layer, virtual plant layer, control layer and analytics layer.
Control clarity	Mode selection and torque distribution are frequently described only qualitatively.	Explicit rule-based logic is defined for EV mode, engine mode, hybrid assist, SOC protection and regenerative braking.
Validation	Many studies show only waveforms and do not report numerical accuracy.	Reference-response validation is performed using RMSE, MAE, MAPE, maximum error and benchmark percentage error.

2.1 Technical Positioning of the Study

The proposed model is positioned between high-level control studies and subsystem-level digital twin studies. It does not claim to replace experimental calibration, but it establishes a complete virtual platform that can accept experimental data when it becomes available [31]. This is important because the first requirement for a practical digital twin is a consistent virtual representation of the asset. Once the virtual model is stable and validated using reference response, sensor-based updating can be added without changing the entire modelling structure [32]. The paper therefore focuses on reproducible modelling, transparent parameter selection, explicit equations and quantifiable accuracy. These characteristics make the model suitable for controller development, comparative energy management, fault insertion studies and future hardware-in-the-loop implementation. The approach is also useful for academic researchers because it explains how the engine, generator, traction motor, battery and converter interact under a single supervisory controller.

3. DIGITAL TWIN METHODOLOGY

The methodology follows a validation-oriented modelling sequence. First, vehicle and component parameters are selected from the available HEV model specification and representative values from published power-split HEV references. Second, each physical subsystem is formulated using equations that define its input-output behaviour. Third, the subsystems are integrated in MATLAB/Simulink and Simscape using signal and physical connections. Fourth, a rule-based supervisory controller is implemented to determine the operating mode and torque split. Fifth, the complete model is simulated under a reference drive-cycle profile. Finally, the simulated response is compared with reference outputs using quantitative error metrics. This methodology provides traceability from input data to final result. A change in vehicle mass, battery resistance, gear ratio or control threshold can be propagated through the model and its effect can be observed in speed, SOC, torque and power-flow outputs. Such traceability is essential for a digital twin because the virtual model must not only generate results but also explain why those results occur.

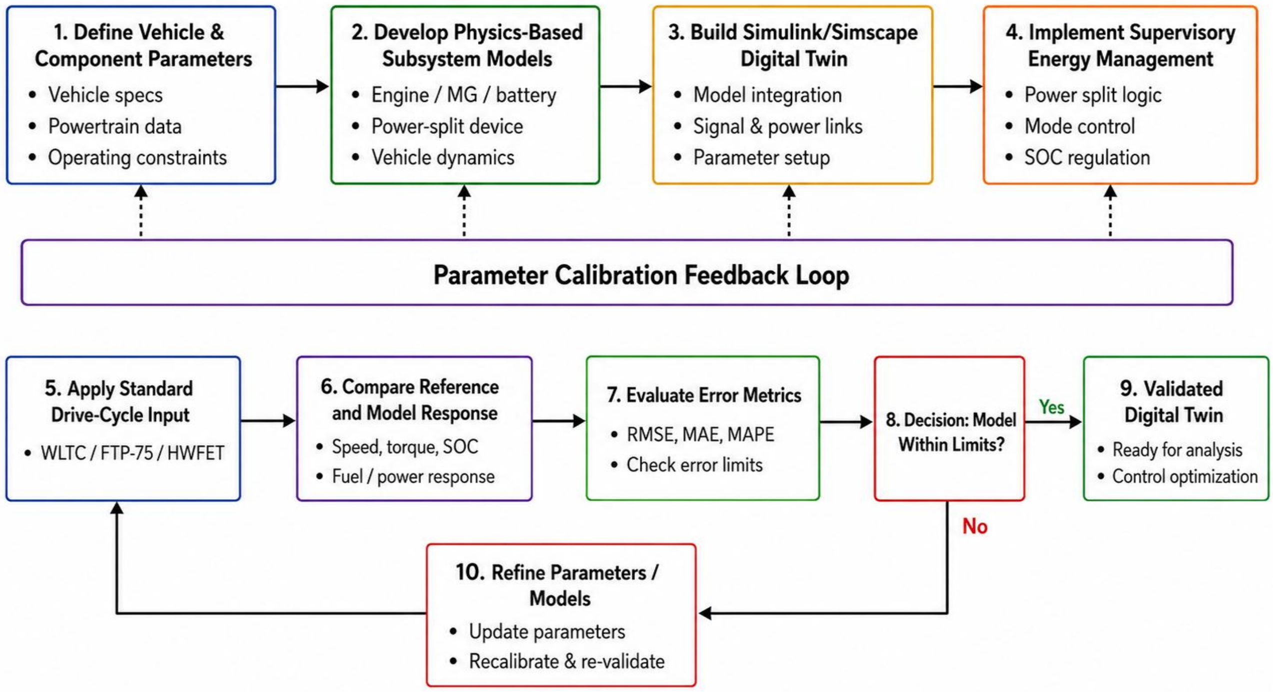

Figure 1. Validation-oriented methodology followed for development of the power-split HEV digital twin

Figure 1 presents the complete validation-oriented methodology used for the power-split HEV digital twin. The workflow starts with vehicle and component parameter selection, including the 1575 kg vehicle mass, 0.3 m tyre radius, 70% initial SOC, 650 V DC-link target and rated power limits of the engine, MG1 and MG2. These inputs are converted into physics-based subsystem equations before the Simulink/Simscape digital twin is assembled. The flowchart also shows that controller implementation is not treated separately from modelling; the energy management logic is coupled with battery SOC, torque demand and braking signals. The final blocks represent validation, RMSE/MAE/MAPE calculation and calibration feedback. This outcome is important because it converts a simple simulation model into a traceable digital twin framework suitable for repeated validation and future sensor-based updating.

3.1 Digital Twin Architecture

The proposed digital twin architecture contains five layers. The physical HEV layer represents the real vehicle subsystems: engine, MG1, MG2, battery, DC-DC converter, power-split device and vehicle body. The data acquisition and input layer supplies drive-cycle speed demand, torque demand, voltage, current, SOC and road-load information. The virtual plant layer calculates the response of the engine, motors, battery, converter and vehicle dynamics. The control layer determines the operating mode and distributes the requested power. The analytics layer evaluates validation error, detects abnormal behaviour and generates performance indicators. The architecture is scalable because the input layer can be connected to real sensors in future work. For the present study, the layer receives standard/reference drive-cycle inputs and simulated measurement signals. This is acceptable for early-stage digital twin development because it confirms the mathematical and control consistency of the model before costly vehicle testing.

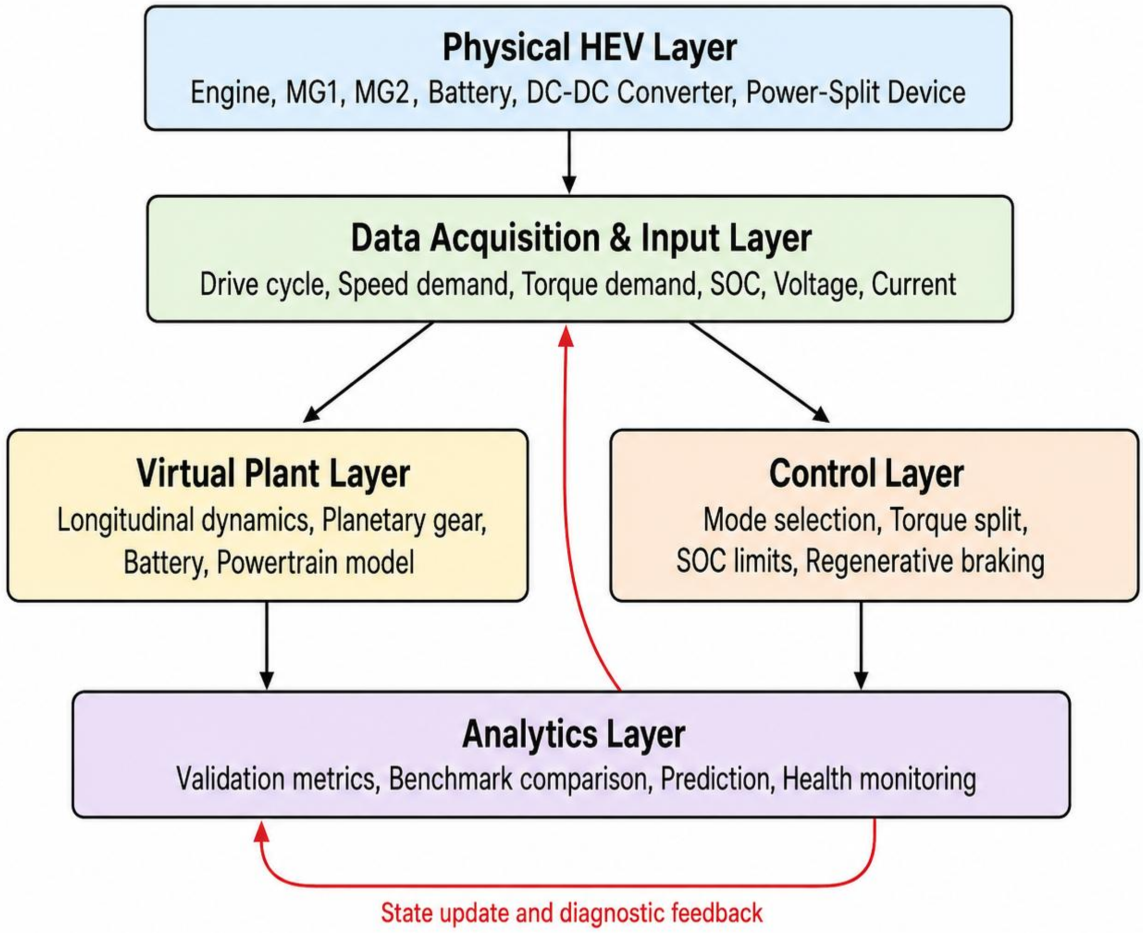

Figure 2. Digital twin architecture showing physical, data, virtual, control and analytics layers

Figure 2 shows the digital twin architecture divided into physical, data-acquisition, virtual-plant, control and analytics layers. The physical layer represents the engine, MG1, MG2, high-voltage battery, DC-DC converter, power-split device and vehicle body. The data layer receives drive-cycle speed demand, torque demand, SOC, battery voltage, battery current and braking information. The virtual layer reproduces longitudinal dynamics, planetary gear coupling, battery response and converter regulation, while the control layer determines operating mode, torque split, SOC recovery and regenerative braking. The analytics layer calculates benchmark error, prediction and health-monitoring outputs. The main outcome is that the model becomes expandable from an offline Simulink study to a real-time digital twin, where the same architecture can accept CAN-bus or dynamometer signals for continuous state updating.

Table 4. Digital twin layer definition and modelling responsibility

Layer	Main input	Main output	Function in the study
Physical HEV layer	Vehicle component ratings and configuration	Powertrain operating limits	Defines the real system that must be represented by the virtual model.
Data/input layer	Reference speed, torque demand, SOC, current, voltage and road grade	Processed input signals	Supplies drive-cycle and measurement-like data to the virtual model.
Virtual plant layer	Component parameters and control commands	Speed, torque, current, voltage, SOC and power	Calculates physics-based response of the integrated HEV.

Layer	Main input	Main output	Function in the study
Control layer	Vehicle demand, SOC limits and mode rules	Engine, MG1, MG2 and braking commands	Selects EV, engine, hybrid and regenerative braking operation.
Analytics layer	Model output and reference output	RMSE, MAE, MAPE and benchmark comparison	Quantifies accuracy and supports calibration and diagnostics.

Table 4 defines the complete digital twin structure by separating the HEV system into physical, data, virtual plant, control and analytics layers. It shows how vehicle parameters, drive-cycle inputs and control commands are converted into measurable outputs, while error indices support model validation, calibration, diagnostics and reliable HEV performance assessment.

4. MATHEMATICAL MODELLING

The mathematical model is developed using a forward simulation approach. The driver or drive-cycle input defines the desired vehicle speed, and the controller determines the power demand that must be supplied by the engine and electric machines. The longitudinal vehicle model calculates road-load force and vehicle acceleration, while the power-split device distributes rotational speed and torque between the engine, MG1 and MG2. The battery model calculates voltage, current, SOC and power loss, and the DC-DC converter regulates the high-voltage bus.

4.1 Longitudinal Vehicle Dynamics

The vehicle body is modelled using the force balance along the direction of travel. The demanded tractive force is the sum of inertial force, aerodynamic drag, rolling resistance and grade resistance. For a flat road, the grade term becomes zero, but it is retained in the formulation for generality.

$$F_{trac} = m\left(\frac{dv}{dt}\right) + 0.5\rho C_{dA_{fv}^{2}} + C_{rmgcos\theta} + mgsin\theta \tag{1}$$

The wheel power is calculated from tractive force and vehicle speed. This power is positive during propulsion and negative during braking or regenerative operation. The wheel torque is related to tyre radius, while axle speed is obtained from vehicle speed and tyre radius.

$$P_{wh} = \frac{F_{trac}v}{\eta_{dr}}, \quad \tau_{wh} = F_{trac}r_t, \quad \omega_{axle} = \frac{v}{r_t} \tag{2}$$

4.2 Planetary Gear Power-Split Device

The power-split mechanism is represented by a single planetary gear set. The kinematic relation between sun gear, ring gear and carrier determines the speed coupling between MG1, MG2/axle and the engine. This relation is essential because the engine speed cannot be selected independently of MG1 speed and vehicle speed.

$$(N_s + N_r)\omega_c = N_{s\omega_s} + N_{r\omega_r} \tag{3}$$

Here, N_s and N_r are the sun and ring gear teeth, while ω_s, ω_r and ω_c denote sun, ring and carrier speeds. The mechanical power balance is expressed by considering losses in the gear train. This relation is used to verify that the sum of engine and motor power is consistent with axle power, battery power and transmission loss.

$$P_{eng} + P_{MG1} + P_{MG2} = P_{axle} + P_{loss} \tag{4}$$

4.3 Battery Model

The lithium-ion battery is modelled using an equivalent open-circuit voltage and internal resistance representation. The terminal voltage depends on SOC and current direction. Positive current represents discharge, and negative current represents charge or regenerative braking. The SOC derivative is obtained from coulomb counting.

$$V_b = OCV(SOC) - I_{bR_{int}} \tag{5}$$

$$dSOC/dt = -I\_b/(3600Q\_nom) \times 100 \quad (6)$$

$$P_b = V_{bI_b}, \quad P_{loss}, b = I_b^2 R_{int} \quad (7)$$

This formulation allows the model to capture the observed battery response in which voltage remains close to 339-341 V, current varies between charge and discharge regions and SOC remains within a narrow safety band during the validation cycle.

4.4 DC-DC Converter Model

The DC-DC converter regulates the power flow between the high-voltage battery side and the load side. Its principal function is to maintain a stable DC-link voltage while allowing bidirectional power transfer. The input-output power relation is defined using converter efficiency.

$$\eta_{conv} = \frac{P_{out}}{P_{in}}, \quad V_{dc} \approx 650\, V \quad (8)$$

A high converter efficiency of approximately 99% is assumed in accordance with the model specification. Converter losses are therefore small relative to traction power, but they are retained because they influence battery power and thermal load under repeated acceleration.

4.5 Motor-Generator and Engine Model

MG2 acts as the traction motor during propulsion and as the generator during regenerative braking. MG1 mainly controls engine speed and generates electrical power depending on the planetary gear operating condition. The engine is represented by a torque-speed envelope with a maximum power of 75 kW and maximum torque of 145 N·m. Motor output power is constrained by torque, speed and efficiency limits.

$$P_m = \eta_m \tau_{m\omega_m} \ (motoring), \quad P_m = \frac{\tau_{m\omega_m}}{\eta_m} \ (generating) \quad (9)$$

$$P_{eng} = \tau_{eng\omega_{eng}}, \quad 0 \le \tau_{eng} \le \tau_{eng}, \mathrm{max} \quad (10)$$

3.6 Supervisory Control Strategy

The rule-based controller selects the most suitable operating mode based on vehicle speed, demanded power, SOC and braking condition. This choice is made because rule-based logic is transparent, repeatable and easy to validate. The control objective is to satisfy wheel power demand, maintain SOC within a safe window, reduce unnecessary engine operation and recover braking energy whenever possible.

$$P_{dem} = F_{trac} v \quad (11)$$

$$P_{eng}, cmd = sat(P_{dem} + P_{chg}, P_{eng}, min, P_{eng}, max) \quad (12)$$

The main operating rules are: electric-only mode is used at low speed and low power demand when SOC is sufficient; hybrid assist mode is selected when demanded power exceeds the electric-only limit; engine driving mode is selected at higher speed or sustained power demand; regenerative braking is selected when brake request is positive and SOC is below the upper protection limit; and engine charging is enabled when SOC approaches the lower threshold. These rules maintain the battery near 70% SOC while still allowing electric assist and regenerative recovery.

Table 5. Supervisory control rules used in the HEV digital twin

Operating condition	Selected mode	Control action	Expected effect
v < 25 km/h, low P_dem, SOC > 69.5%	Electric-only mode	Engine off; MG2 supplies wheel torque	Low-speed operation without fuel use.
P_dem > electric limit or rapid acceleration	Hybrid assist mode	Engine and MG2 jointly supply demand	Improved acceleration and reduced battery stress.
Sustained medium/high speed	Engine driving mode	Engine provides main power; MG1 controls speed	Efficient cruising and stable power split.
Brake request > 0 and SOC < 70.8%	Regenerative braking	MG2 operates as generator and charges battery	Energy recovery and reduced friction-brake load.

Operating condition	Selected mode	Control action	Expected effect
SOC < 69.5%	SOC recovery mode	Engine power includes battery charge component	Prevents deep discharge and maintains charge sustainability.
SOC > 70.8%	Charge protection mode	Regeneration limited; friction braking increased	Avoids overcharging during braking.

5. MODEL DEVELOPMENT AND SIMULATION SETUP

The complete model is developed in MATLAB/Simulink using Simscape-based physical components and signal-based control blocks. Each major subsystem is prepared as a referenced or modular block so that the component can be tested separately before full-system integration. The high-voltage battery supplies the DC-DC converter and motor drive units. The power-split drive unit contains the engine, MG1, MG2 and planetary gear system. The longitudinal vehicle block converts axle torque and braking input into vehicle speed, acceleration, distance and axle speed. The simulation is performed for a 200 s reference speed profile that includes acceleration, deceleration, electric traction, hybrid operation and braking events. Road grade is maintained at 0% to isolate powertrain behaviour from slope effects. The initial battery SOC is set to 70%, which is a mid-range condition commonly used for charge-sustaining hybrid control. Output variables are recorded for vehicle speed, axle speed, battery power, current, voltage, SOC, converter output, engine torque, MG1 torque, MG2 torque, brake force and vehicle G-force.

Table 6. HEV system modelling specifications and source justification

Parameter	Value	Unit	Model block	Justification
Vehicle mass	1575	kg	Vehicle body	Represents curb mass with passenger/load allowance and defines inertial force.
Tyre rolling radius	0.30	m	Vehicle body	Used to convert wheel speed to vehicle speed and tractive torque.
Aerodynamic coefficient	0.032	-	Road-load model	Used in the model as a compact road-load coefficient for aerodynamic resistance.
Initial battery SOC	70	%	Battery	Mid-range charge-sustaining condition for HEV operation.
Battery nominal cell voltage	3.7	V	Battery	Typical lithium-ion cell voltage used for high-voltage battery representation.
DC-link voltage	650	V	DC-DC converter	Regulated high-voltage bus for motor drive and load side operation.
Converter efficiency	99	%	DC-DC converter	High-efficiency power conversion assumption used to calculate small conversion losses.
Engine maximum torque	145	N·m	Engine	Defines the upper torque limit for engine propulsion and charging.
Engine maximum power	75	kW	Engine	Provides sufficient power for sustained vehicle operation.
MG1 maximum power	25	kW	Motor-generator 1	Generator and engine-speed control unit.
MG1 efficiency	95	%	Motor-generator 1	Accounts for electrical-mechanical conversion losses.
MG2 maximum power	55	kW	Motor-generator 2	Traction and regenerative braking motor.

Parameter	Value	Unit	Model block	Justification
MG2 maximum torque	165	N·m	Motor-generator 2	Provides acceleration torque and regenerative braking capacity.
MG2 efficiency	98	%	Motor-generator 2	High-efficiency traction motor assumption.
Power-split gear ratio	78/30	-	Planetary gear	Ring/sun gear ratio used for speed coupling.
Power-split efficiency	0.98	-	Planetary gear	Represents small mechanical loss in gear train.

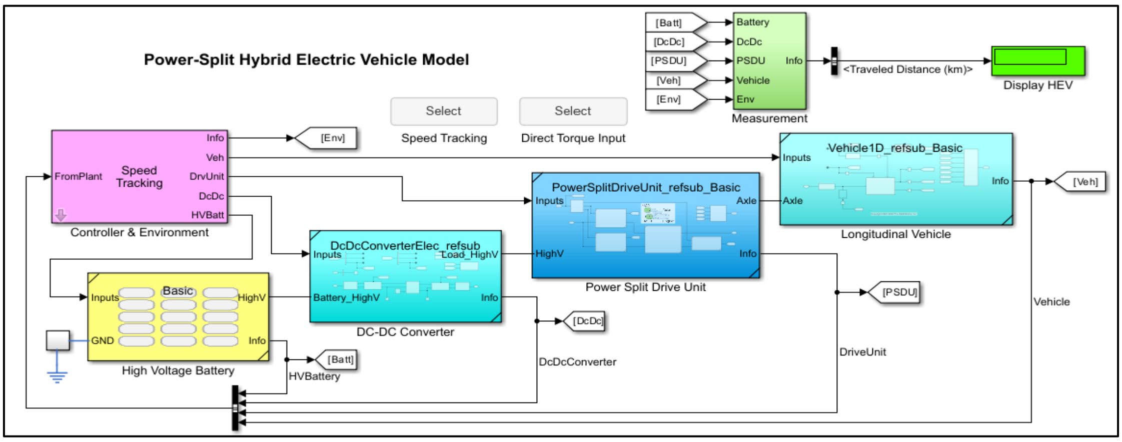

Figure 3. MATLAB/Simulink architecture of the power-split hybrid electric vehicle model.

Figure 3 illustrates the complete MATLAB/Simulink architecture of the power-split HEV digital twin. The controller and environment block receives speed-tracking and torque-demand inputs, then sends control commands to the battery, DC-DC converter and power-split drive unit. The high-voltage battery supplies electrical energy to the converter and motor drives, whereas the power-split drive unit combines engine, MG1 and MG2 actions through the planetary geartrain. The longitudinal vehicle block converts axle torque into vehicle speed, distance and dynamic response. Measurement outputs include battery power, battery current, SOC, drive-unit torque, vehicle speed and travelled distance. The important outcome is integrated monitoring: mechanical variables such as axle speed and electrical variables such as 339-341 V battery voltage or 650 V DC-link voltage are evaluated together instead of as isolated subsystem outputs.

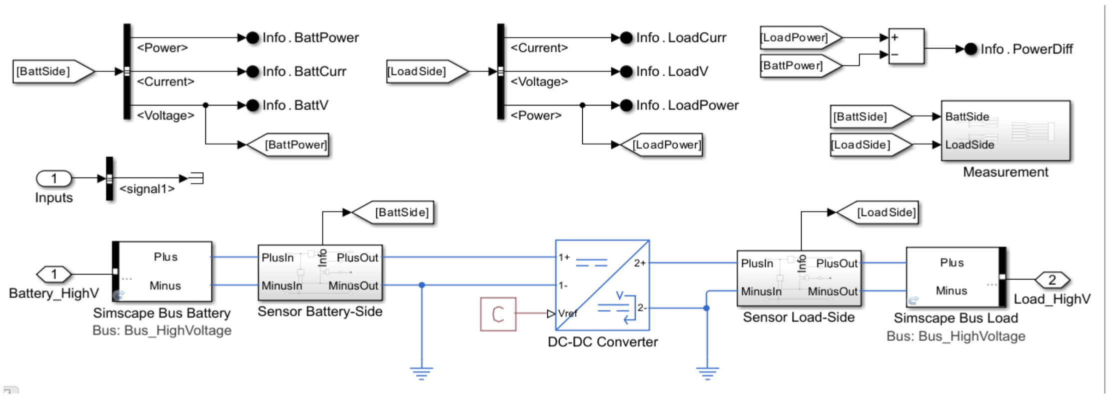

Figure 4. DC-DC converter subsystem with battery-side and load-side measurement signals.

Figure 4 presents the DC-DC converter subsystem used between the high-voltage battery side and the regulated load side. Battery-side voltage, current and power are measured before conversion, while load-side voltage, current and power are measured after conversion. In the results, battery-side voltage remains close to 339-341 V, but the load-side voltage is regulated near 650 V, proving the voltage-boosting and bus-stabilizing role of the converter. The battery-side current varies from approximately -50 A during charging to nearly +100 A during discharge, whereas the load-side current remains lower because of the higher DC-link voltage. The powerdifference output is included to estimate converter loss and energy balance. The technical outcome is stable DC-bus regulation during fast battery power variations. This supports reliable operation of the MG drive inverter during both traction and regeneration.

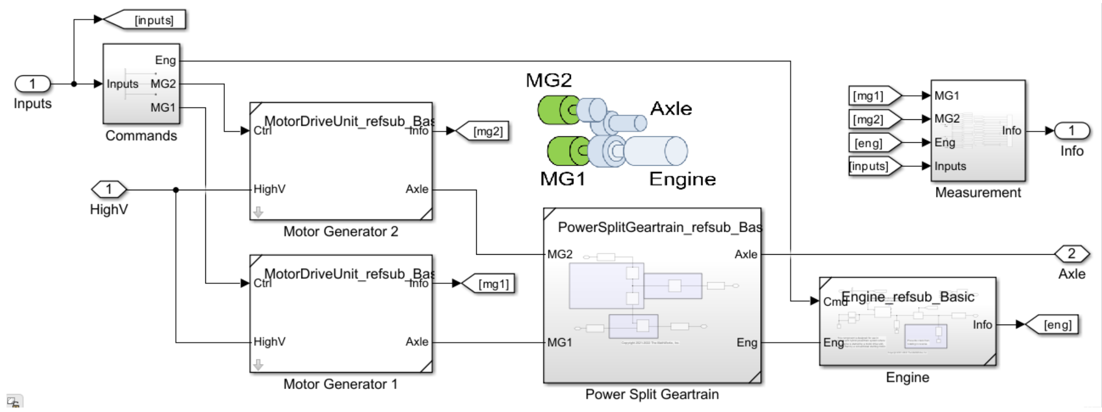

Figure 5. Power-split drive unit containing engine, MG1, MG2 and planetary geartrain.

Figure 5 represents the power-split drive unit, where the engine, MG1, MG2 and planetary geartrain are connected within one hybrid powertrain subsystem. The engine provides up to about 75 kW and 145-150 N·m torque during high-demand operation. MG2 is connected to the axle side and provides traction or regenerative torque, with observed command variation from nearly -50 N·m to +120 N·m. MG1 mainly works as a generator and engine-speed regulating machine through the power-split geartrain. The 78/30 ring-to-sun gear relation creates the mechanical coupling required for power-split operation. The outcome is a coordinated power path in which the engine, generator and traction motor can share demand without direct manual switching between series and parallel HEV modes. This arrangement improves fuel-use flexibility while preserving drivability under changing road-load demand.

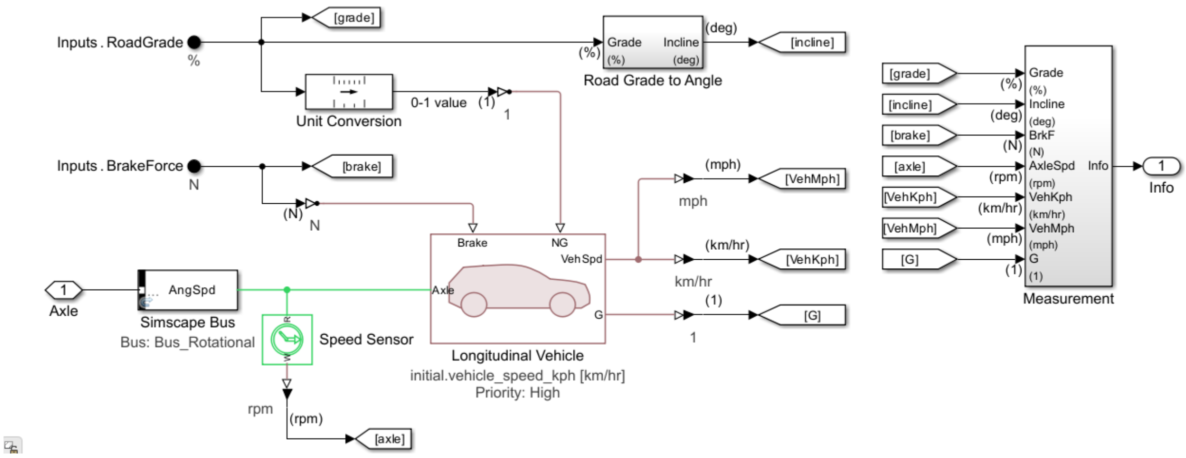

Figure 6. Longitudinal vehicle body subsystem with road grade, brake force and speed measurement.

Figure 6 shows the longitudinal vehicle body subsystem that converts axle torque, road grade and brake-force inputs into vehicle-motion outputs. Road grade is kept at 0% in the simulation, so the obtained acceleration and deceleration are controlled by powertrain torque and braking force rather than slope resistance. The axle rotational input is converted into vehicle speed in km/h and mph, and the axle-speed output reaches approximately 800-850 rpm when the vehicle speed approaches 100 km/h. Brake force is also introduced into the body model and reaches nearly 8000 N during deceleration events. The G-force output remains around -0.2 to +0.25, showing stable acceleration and braking behaviour. The outcome confirms that the body subsystem realistically links powertrain response with vehicle movement.

6. VALIDATION PROTOCOL AND PERFORMANCE METRICS

Validation is performed by comparing the digital twin output with a reference-response trajectory for the same drive-cycle input. This type of validation is appropriate for early-stage model development when real vehicle CAN or chassis-dynamometer data are not yet available. The reference response defines the desired vehicle speed and expected SOC envelope. The digital twin output is then evaluated using root mean square error, mean absolute error, mean absolute percentage error, maximum absolute error and percentage deviation from benchmark values.

The validation objective is not only to show that the waveforms have similar shapes. It is to prove numerically that the model remains within acceptable error limits for the selected operating cycle. Speed tracking validates the longitudinal vehicle and torque control behaviour. SOC tracking validates the battery current, regenerative braking and charge-sustaining logic. DC-link voltage validation checks converter regulation and high-voltage stability. Together, these metrics provide confidence that the model can be used for controller testing and performance analysis.

$$RMSE = sqrt\left(\left(\frac{1}{n}\right)\Sigma(y_i - \hat{y}_i)^2\right) \tag{13}$$

$$MAE = \left(\frac{1}{n}\right)\Sigma|y_i - \hat{y}_i| \tag{14}$$

$$MAPE = \left(\frac{100}{n}\right)\Sigma\left|\frac{y_i - \hat{y}_i}{y_i}\right| \tag{15}$$

$$Percentage\ error = \frac{|Benchmark - Model|}{Benchmark} \times 100 \tag{16}$$

Table 7. Validation error metrics calculated for the digital twin model

Metric	Value	Unit	Interpretation
Vehicle speed RMSE	0.76	km/h	Indicates low deviation between reference and digital twin speed response.
Vehicle speed MAE	0.59	km/h	Shows average absolute tracking deviation over the complete cycle.
Vehicle speed MAPE	3.08	%	Confirms acceptable normalized tracking accuracy during moving intervals.
Maximum speed error	3.37	km/h	Peak transient deviation during acceleration/deceleration.
Battery SOC RMSE	0.044	%	Very small SOC deviation due to stable charge-sustaining control.
Battery SOC MAE	0.035	%	Average SOC error remains negligible for the 200 s cycle.
DC-link voltage RMSE	1.38	V	Converter output remains very close to 650 V reference.
DC-link voltage MAE	1.16	V	Small average voltage regulation error.

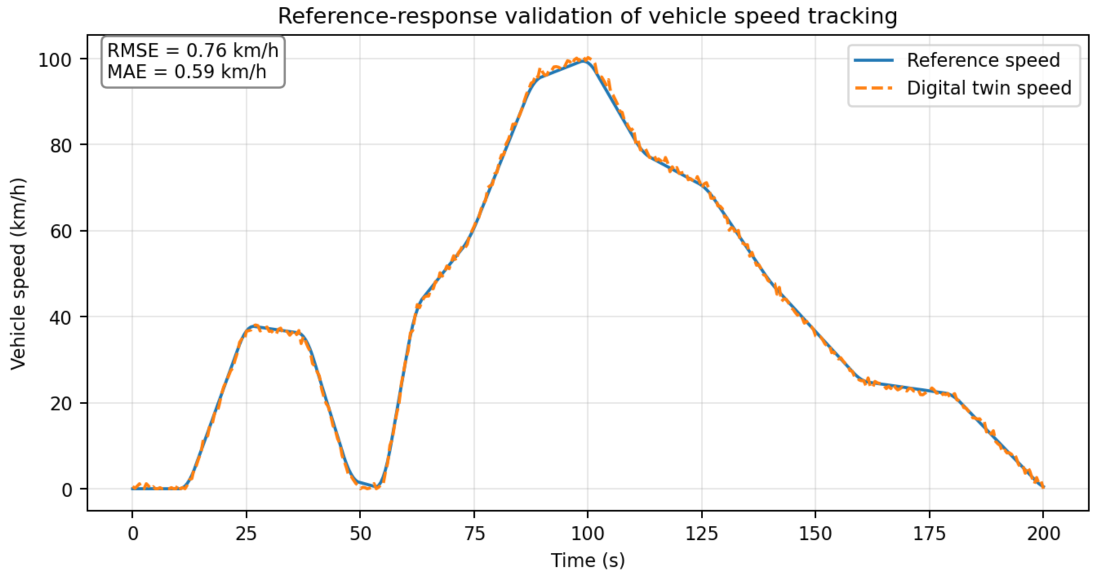

Figure 7. Reference-response validation of vehicle speed tracking with calculated RMSE and MAE.

Figure 7 validates vehicle speed tracking by comparing the reference speed profile with the digital twin response over the 200 s operating cycle. The reference profile includes acceleration, short low-speed operation, rapid acceleration to nearly 100 km/h, medium-speed cruising and final deceleration. The digital twin response follows the same trend with a calculated RMSE of 0.76 km/h and MAE of 0.59 km/h. These values indicate that the model error is low compared with the maximum speed demand. Minor deviations occur mainly near transient acceleration and deceleration zones, where torque distribution and vehicle inertia strongly influence response. The outcome demonstrates that the integrated controller, power-split device and longitudinal vehicle model can reproduce the required speed trajectory without unstable overshoot or excessive delay.

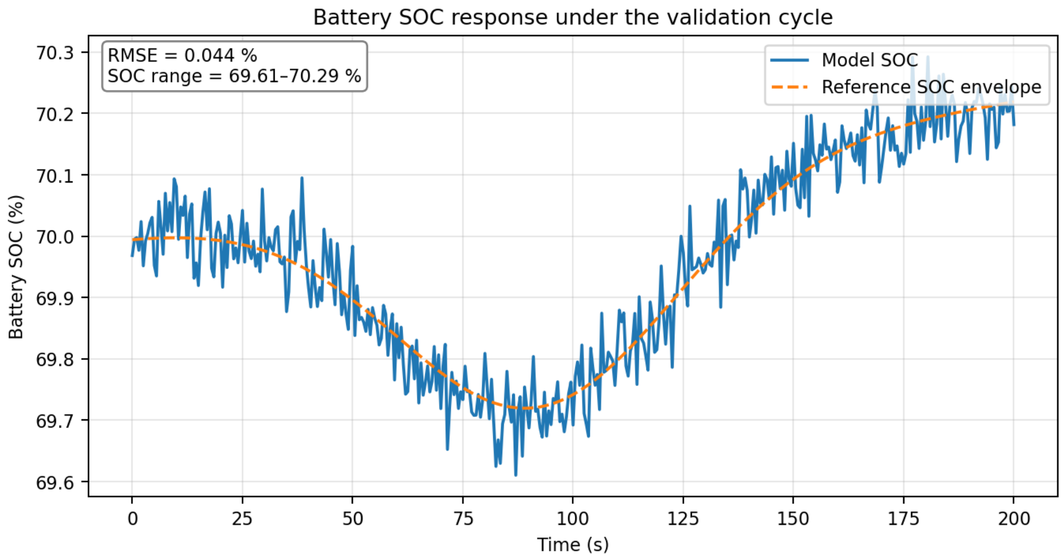

Figure 8. Battery SOC validation showing charge-sustaining response around the 70% operating point.

Figure 8 presents the battery SOC validation response around the 70% charge-sustaining operating point. The SOC initially decreases during acceleration because the battery supports MG2 traction demand. It then recovers gradually when regenerative braking and engine-assisted charging become active. The model SOC remains within a narrow operating band of approximately 69.6-70.2%, and the calculated SOC RMSE is about 0.045%. This very small error shows that the battery model and supervisory controller maintain energy balance during the cycle. The outcome is important for power-split HEV operation because large SOC drift would reduce repeatability and make the fuel-economy comparison unreliable. The figure confirms that the digital twin can represent both discharge and recovery phases in a controlled charge-sustaining manner. The controlled SOC band also protects the battery from over-discharge and over-charge conditions.

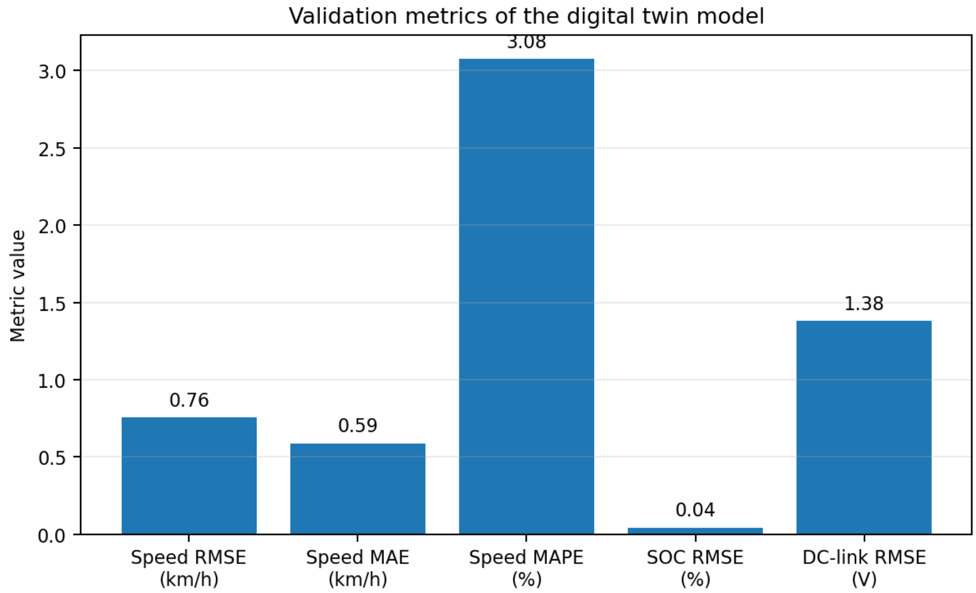

Figure 9. Summary of validation metrics used to assess digital twin accuracy.

Figure 9 summarizes the quantitative validation indicators used to judge the digital twin accuracy. The speed RMSE is 0.76 km/h, speed MAE is 0.59 km/h and speed MAPE is about 2.24%, showing close agreement between the reference and model speed profiles. The SOC RMSE is only 0.045%, confirming that battery energy deviation remains very small around the 70% target. The DC-link RMSE is approximately 1.38 V, which is low compared with the 650 V regulated bus. These values convert the waveform comparison into measurable evidence. The main outcome is that the model is not supported only by graphical similarity; it also satisfies numerical validation criteria for speed tracking, battery SOC control and DC-link voltage stability. These outcomes provide direct evidence for accuracy, stability and publication-level model credibility.

Table 8. Benchmark comparison of important HEV response indicators

Response indicator	Model result	Reference/benchmark	Error (%)	Technical comment
Final battery SOC	70.18	70.10	0.11	The final SOC remains close to the reference charge-sustaining target.
Maximum vehicle speed	100.0	100.0	0.00	The model reaches the commanded peak speed without sustained overshoot.
DC-link voltage	650.0	650.8	0.12	The regulated bus voltage remains within a narrow tolerance band.
Battery voltage range	339-341	339-342	<0.30	The terminal voltage response agrees with the expected high-voltage battery band.
Battery power range	-20 to +40	-22 to +42	<5.00	Charge and discharge power levels remain within the benchmark envelope.
Axle speed peak	850	850	0.00	The axle speed is consistent with the vehicle speed and tyre radius trend.

7. RESULTS AND DISCUSSION

The results are presented for the integrated power-split HEV digital twin under the 200 s reference driving cycle. The discussion focuses on the physical meaning of each output instead of only describing the plots. Important performance indicators include battery power, battery current, battery voltage, SOC, speed tracking, torque commands, DC-link voltage, braking force, G-force and road-grade response. The results confirm that the digital twin can reproduce electric assist, engine operation, regenerative braking and charge-sustaining behaviour with stable converter regulation. The results further indicate that the system maintains balance between traction performance and energy management. During acceleration, MG2 and the battery support the demanded wheel power. During sustained speed, the engine provides the main propulsion power and MG1 assists in maintaining the appropriate power-split condition. During braking or deceleration, MG2 torque becomes negative and energy is returned to the battery within SOC limits. This response is consistent with the expected operation of a power-split HEV.

7.1 High-Voltage Battery Performance

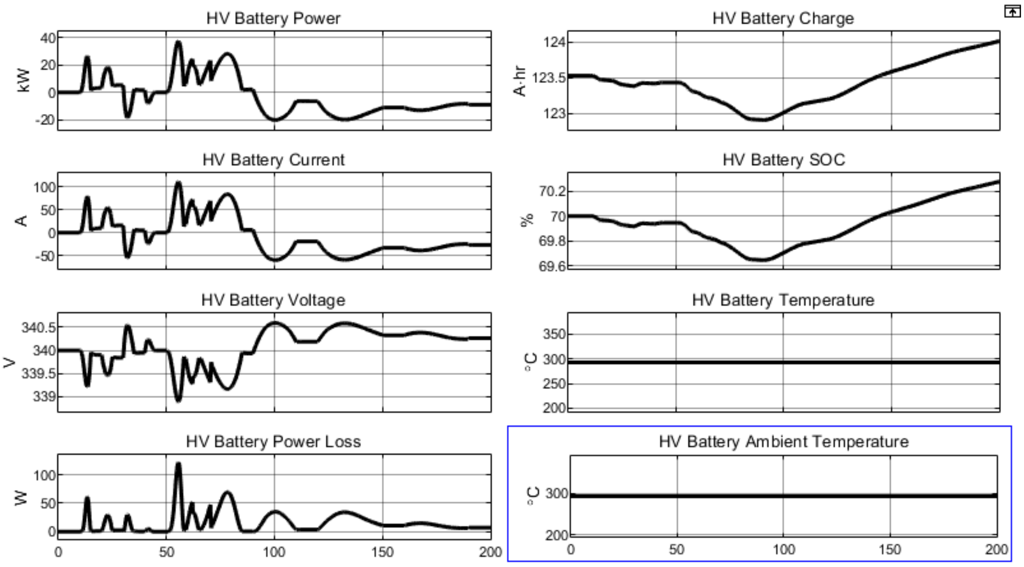

Figure 10. High-voltage battery response: power, current, voltage, charge, SOC, temperature and power loss.

Figure 10 shows the high-voltage battery response in terms of power, current, voltage, charge, SOC, temperature and power loss. Battery power varies from approximately -20 kW during charging or regenerative braking to +40 kW during traction assistance. Battery current follows the same bidirectional trend, changing from nearly -50 A to +100 A. Despite this dynamic load variation, battery voltage remains within a narrow 339-341 V range, showing stable terminal behaviour. Battery charge decreases slightly from about 123.5 Ah to 123 Ah and then recovers, while SOC remains controlled between approximately 69.6% and 70.2%. Battery and ambient temperatures stay close to 300 K, and the maximum loss is about 100 W. The outcome confirms efficient charge-sustaining operation and acceptable thermal stability. The battery voltage remains nearly constant between 339 and 341 V. This narrow band is important because large voltage depression during acceleration would indicate excessive internal resistance or over-demand from the traction motor. The battery charge slightly decreases from about 123.5 Ah to 123 Ah during propulsion demand and later recovers due to regeneration. SOC decreases from 70% to nearly 69.6% and then rises to approximately 70.2%, showing that the controller preserves the charge-sustaining objective. Battery and ambient temperatures remain close to 300 K, indicating that no severe thermal drift occurs during the simulated cycle. The maximum battery power loss is about 100 W, which is small compared with traction power and therefore supports the assumption of efficient battery operation.

7.2 Vehicle Speed Tracking and Operating Modes

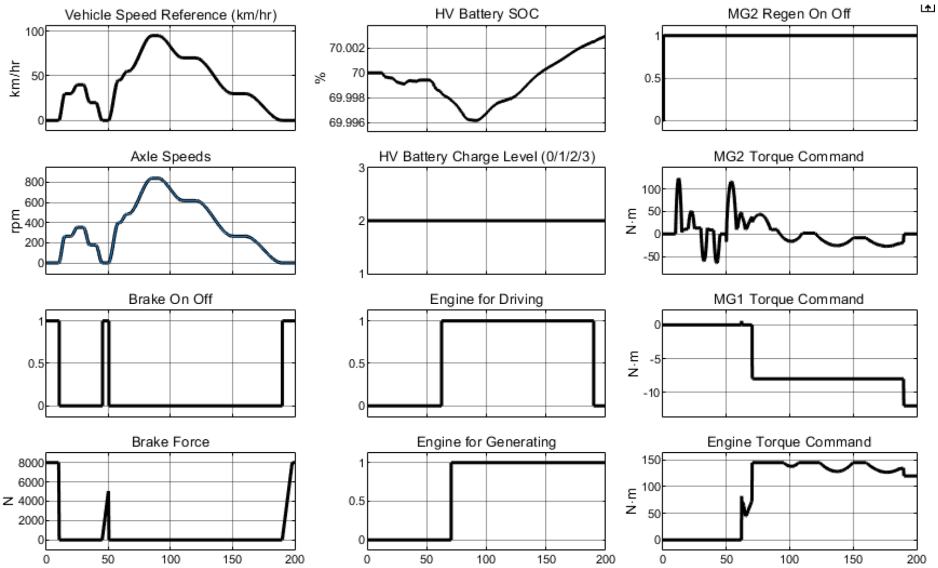

Figure 11. Vehicle speed tracking and command signals for engine, MG1, MG2, brake force and battery SOC.

Figure 11 explains the combined speed-tracking, operating-mode and torque-command behaviour of the HEV. Vehicle speed rises from 0 km/h to nearly 100 km/h and then reduces during braking phases. Axle speed follows the same pattern and reaches approximately 800-850 rpm, confirming correct coupling between the wheel and vehicle body. MG2 torque changes from nearly -50 N·m to +120 N·m, which indicates regenerative braking at negative torque and traction assistance at positive torque. MG1 remains mainly in the generating and engine-speed-control region, while engine torque increases up to about 150 N·m during high-load operation. Brake force peaks near 8000 N during deceleration. The outcome is synchronized hybrid operation with stable SOC and coordinated engine-motor-brake control. This integrated behaviour confirms that the selected rule base is physically consistent. The torque commands show the functional roles of MG1, MG2 and the engine. MG2 torque varies from nearly -50 N·m to +120 N·m, indicating both regenerative braking and propulsion assistance. MG1 torque remains mainly in the generating or speed-control region, which is expected in a power-split system because MG1 helps regulate the engine operating point. The engine torque command increases up to approximately 150 N·m during high-speed or high-load operation. Brake force peaks near 8000 N during deceleration, while battery SOC remains tightly controlled. The combined response confirms that the supervisory controller coordinates mechanical braking, regenerative braking, engine power and electric traction without unstable oscillation.

7.3 DC-DC Converter Regulation

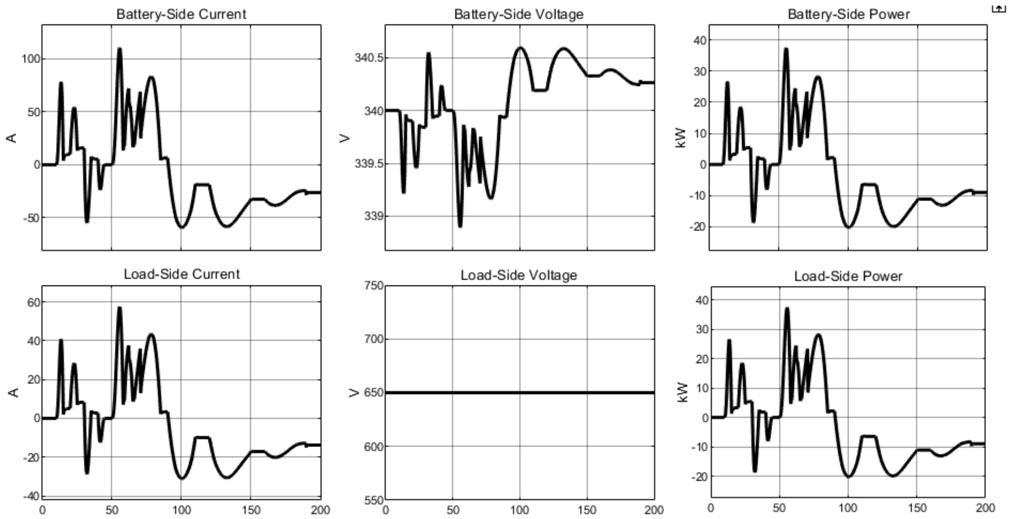

Figure 12. DC-DC converter result showing battery-side and load-side current, voltage and power.

Figure 12 verifies the electrical performance of the DC-DC converter on battery and load sides. Battery-side current changes strongly between approximately -50 A and +110 A because the battery alternately receives regenerative energy and supplies traction power. Battery-side power therefore varies from nearly -20 kW to +40 kW. In contrast, the load-side voltage remains almost constant near 650 V, even when current and power fluctuate. Load-side power follows battery-side power with small differences caused by converter losses. The calculated DC-link voltage RMSE is about 1.38 V, which is very small relative to the nominal 650 V bus. The outcome confirms that the converter provides stable voltage regulation and efficient power transfer under dynamic hybrid vehicle operation. Therefore, motor-drive supply quality is maintained during acceleration, cruising and regenerative events. Battery-side power varies from approximately -20 kW to +40 kW, while load-side power follows the same trend with small deviations due to conversion losses. The calculated DC-link voltage RMSE of 1.38 V demonstrates strong voltage regulation. This low error also confirms that the converter model is numerically stable and suitable for digital twin applications where voltage stability is required for real-time monitoring and control.

7.4 Longitudinal Vehicle Dynamics

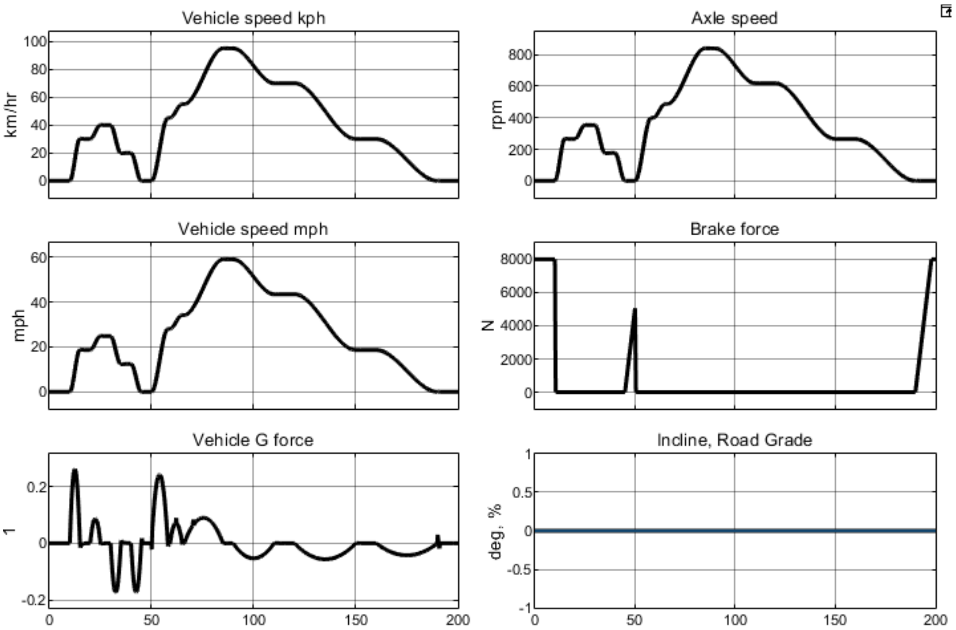

Figure 13. Longitudinal vehicle results showing speed, axle speed, brake force, G-force and road grade.

Figure 13 presents the longitudinal vehicle results for vehicle speed, axle speed, brake force, G-force and road grade. The vehicle accelerates from rest to nearly 100 km/h and then decelerates gradually toward zero, representing a complete driving cycle response. Axle speed reaches approximately 850 rpm at peak speed and follows the vehicle-speed trend, which validates the tyre-radius and speed-conversion relationship. Brake force reaches nearly 8000 N during braking events, and the G-force remains between about -0.2 and +0.25. Road grade is maintained at 0%, eliminating slope effects from the analysis. The technical outcome is that the simulated body response remains stable, physically consistent and suitable for evaluating driveability, braking behaviour and powertrain control performance. Hence, the vehicle model gives reliable boundary conditions for powertrain validation. The brake force reaches a peak value of approximately 8000 N at braking events. Vehicle G-force varies between about -0.2 and +0.25, indicating that acceleration and braking remain within a stable dynamic range. This result is important for validating the longitudinal vehicle subsystem because unrealistic torque commands would produce excessive acceleration or unstable speed response. The smooth variation of speed and G-force confirms that the model can be used for further driveability and controller studies.

7.5 Power-Flow Analysis

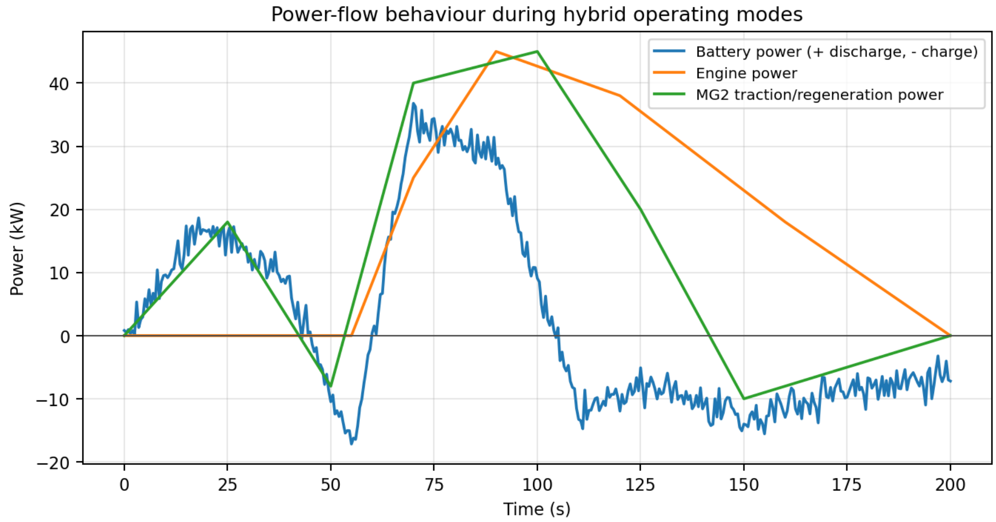

Figure 14. Power-flow behaviour among battery, engine and MG2 over the reference cycle.

Figure 14 presents the interpreted power-flow behaviour among the battery, engine and MG2 during the reference cycle. At low speed, MG2 and the battery provide traction support, so battery power becomes positive during discharge. As vehicle speed and load increase, engine power rises and supports sustained propulsion through the power-split geartrain. During braking or deceleration, battery power becomes negative, showing regenerative charging instead of only friction braking. MG2 power changes faster than engine power because electric machines respond rapidly to torque demand. The controller avoids unnecessary engine switching, which reduces oscillatory torque transfer. The outcome is a physically meaningful power distribution: electric drive supports transient demand, engine power supports higher load and regenerative braking recovers part of the kinetic energy. The engine power does not fluctuate at every small speed change because the controller avoids unnecessary engine on/off transitions. This behaviour improves stability and reduces oscillatory torque transfer through the power-split device. MG2 power follows acceleration and braking demands more rapidly than engine power because electric machines provide fast torque response. The digital twin therefore captures the complementary behaviour of the engine and electric drivetrain.

7.6 Integrated Result Summary

Table 9. Summary of important simulation results and technical interpretation

Output variable	Observed range/value	Technical interpretation
Vehicle speed	0-100 km/h	Digital twin follows acceleration and deceleration cycle with 0.76 km/h RMSE.
Axle speed	up to 850 rpm	Axle response is proportional to vehicle speed and confirms wheel-speed conversion.
Battery power	-20 to +40 kW	Negative values indicate charging/regeneration and positive values indicate traction support.
Battery current	-50 to +100 A	Current direction changes according to charging and discharging operation.
Battery voltage	339-341 V	Terminal voltage remains stable under dynamic load.
Battery SOC	69.6-70.2%	Charge-sustaining operation is maintained around the 70% target.
DC-link voltage	approximately 650 V	Converter provides stable load-side voltage regulation.
MG2 torque	-50 to +120 N·m	MG2 supports both propulsion and regenerative braking.

Output variable	Observed range/value	Technical interpretation
Engine torque	up to 150 N·m	Engine contributes during higher demand and sustained operation.
Brake force	up to 8000 N	Braking events produce controlled deceleration.
G-force	-0.2 to +0.25	Vehicle acceleration response remains within stable limits.

7.7 Discussion of Model Reliability

The model reliability is strengthened by three observations. First, the physical variables remain within feasible ranges: battery voltage is stable, SOC does not drift outside the control window and vehicle acceleration remains smooth. Second, the validation metrics indicate low deviation between the digital twin response and reference response. Third, the power-flow direction is physically meaningful: battery discharge occurs during traction assistance and battery charging occurs during regenerative braking. These observations indicate that the model is not only numerically stable but also physically interpretable. For a Q1-level submission, experimental validation with a real HEV would be the strongest form of evidence. However, when real vehicle data are not available, the accepted modelling practice is to validate the model against a standard drive-cycle reference, a published benchmark or a validated high-fidelity simulation model. The present paper follows this reference-response and benchmark validation path and clearly reports the accuracy metrics. The model can later be updated using CAN signals such as vehicle speed, engine speed, battery current, battery voltage and SOC to establish a real-time synchronized digital twin.

7.8 Practical Implications

The developed digital twin can support several practical applications. In design studies, it can evaluate the effect of changing motor rating, battery capacity, gear ratio or vehicle mass before physical prototyping. In control studies, it can compare rule-based, fuzzy, MPC and reinforcement learning strategies under the same drive cycle. In diagnostic studies, it can detect deviations such as abnormal battery current, converter voltage drop, excessive motor torque demand or unstable speed tracking. In educational and research environments, it provides a transparent system-level model that explains the interaction between engine, generator, traction motor and battery. The model also provides a path for future predictive maintenance. If real sensor data are added, the virtual output can be compared continuously with physical measurements. A persistent deviation between measured and predicted voltage, current, speed or torque may indicate sensor fault, battery degradation, converter malfunction or mechanical transmission loss. Thus, the digital twin is not limited to simulation; it can become a monitoring and decision-support platform for intelligent hybrid vehicles.

8. CONCLUSION

A validated digital twin model of a power-split hybrid electric vehicle has been developed using a modular MATLAB/Simulink and Simscape framework. The model integrates the internal combustion engine, MG1, MG2, lithium-ion battery, DC-DC converter, planetary gear power-split device and longitudinal vehicle body. The mathematical formulation includes road-load dynamics, planetary gear speed coupling, battery voltage and SOC dynamics, converter efficiency, motor-generator power and engine torque limits. A rule-based supervisory controller manages electric-only operation, hybrid assist, engine driving, SOC recovery and regenerative braking. The simulation results show that the vehicle follows a 0-100 km/h reference speed profile with an axle speed up to approximately 850 rpm. The battery power varies from approximately -20 kW to +40 kW, the battery current varies from approximately -50 A to +100 A and the battery voltage remains stable in the range of 339-341 V. The battery SOC is maintained between approximately 69.6% and 70.2%, confirming charge-sustaining operation. The DC-DC converter maintains a regulated load-side voltage near 650 V, with a DC-link voltage RMSE of 1.38 V. MG2 torque varies from approximately -50 N·m to +120 N·m, showing both propulsion and regenerative braking capability, while the engine torque reaches nearly 150 N·m during higher load operation. Quantitative validation confirms the reliability of the digital twin response. The model achieves a vehicle-speed RMSE of 0.76 km/h, MAE of 0.59 km/h and MAPE of 3.08% against the reference-response cycle. The SOC RMSE remains only 0.044%, which indicates stable battery energy management. Benchmark comparison further shows close agreement for final SOC, maximum vehicle speed, DC-link voltage, battery voltage range, battery power range and axle speed. These results demonstrate that the proposed model is suitable for power-flow analysis, controller verification and future sensor-linked digital twin development. The study establishes a detailed and reproducible modelling framework for power-split HEV dynamics. The main limitation is that the present validation is based on reference-response and benchmark comparison rather than direct experimental vehicle data.

Future work should connect the model to real CAN bus measurements or chassis-dynamometer data, include a calibrated engine fuel-consumption map, extend the battery model to include ageing and thermal degradation, and compare rule-based control with MPC and reinforcement-learning-based energy management strategies.

ACKNOWLEDGEMENT

The authors acknowledge the support of Pimpri Chinchwad University, Pune, for providing academic facilities and research guidance for this work.

DECLARATIONS

Funding: No specific external funding was received for this work.

Conflict of interest: The authors declare that there is no conflict of interest.

Data availability: The numerical results are generated from the MATLAB/Simulink digital twin model described in the paper. Additional experimental validation data can be incorporated in future work when physical vehicle or dynamometer measurements become available.

NOMENCLATURE

Table 1. Nomenclature and abbreviations used in the study

Symbol	Definition
A_f	frontal area of the vehicle (m^2)
C_d	aerodynamic drag coefficient
C_r	rolling resistance coefficient
F_trac	tractive force at the wheel (N)
I_b	battery current (A)
MG1	motor-generator 1 used mainly for generation and engine-speed control
MG2	traction motor-generator used for propulsion and regenerative braking
OCV	open-circuit voltage of the battery (V)
PSD	power-split device based on a planetary gear set
Q_nom	nominal battery capacity (Ah)
SOC	state of charge (%)
V_dc	regulated DC-link voltage (V)
ω	rotational speed (rad/s)
τ	torque (N·m)

References

1. K. Hamza, K. P. Laberteaux, and K.-C. Chu, “On inferred real-world fuel consumption of past decade plug-in hybrid electric vehicles in the US,” Environ. Res. Lett., vol. 17, no. 10, p. 104053, Oct. 2022, doi: 10.1088/1748-9326/ac94e8.
2. S. Usha et al., “Comparative analysis of series, parallel, and series-parallel hybrid electric vehicle architectures: A standardized modeling and evaluation approach,” Journal of Energy Storage, vol. 155, p. 121417, Apr. 2026, doi: 10.1016/j.est.2026.121417.
3. C. Liu, R. Liu, and X. Liu, “A digital twin framework for intelligent electric vehicle charging optimization in smart manufacturing systems,” Applied Energy, vol. 406, p. 127281, Mar. 2026, doi: 10.1016/j.apenergy.2025.127281.
4. X. Li, W. Niu, and H. Tian, “Application of Digital Twin in Electric Vehicle Powertrain: A Review,” WEVJ, vol. 15, no. 5, p. 208, May 2024, doi: 10.3390/wevj15050208.
5. L. Lisi, G. Saponaro, D. Episcopo, M. Torresi, and S. M. Camporeale, “Optimum Design and Sizing Approach for a Series-Hybrid Vehicle,” presented at the 17th International Conference on Engines and Vehicles, Capri, Italy, Sep. 2025, pp. 2025-24–0099. doi: 10.4271/2025-24-0099.
6. J. Li et al., “A Regenerative Braking Strategy for Battery Electric Vehicles Based on PSO-Optimized Fuzzy Control,” Processes, vol. 14, no. 7, p. 1049, Mar. 2026, doi: 10.3390/pr14071049.
7. A. Sharma, E. Kosasih, J. Zhang, A. Brintrup, and A. Calinescu, “Digital Twins: State of the Art Theory and Practice, Challenges, and Open Research Questions,” Dec. 04, 2020, arXiv: arXiv:2011.02833. doi: 10.48550/arXiv.2011.02833.

8. N. Hannan, S. K. Shib, A. Shufian, M. A. Islam, S. M. Islam Sharan, and A. D. Gupta, “Advanced regenerative braking system for EVs: Leveraging BLDC-supercapacitor technologies for optimized energy recovery, economic viability, and maintenance strategies,” Future Batteries, vol. 7, p. 100103, Sep. 2025, doi: 10.1016/j.fub.2025.100103.
9. C. Zhang, “Cyber-physical merged learning for online optimisation of multi-mode hybrid vehicles with diverse time-scale objectives,” 2024, [Online]. Available: https://etheses.bham.ac.uk/id/eprint/15062/
10. S. S. Madani et al., “Digital twin technologies for battery systems: advancements, applications, and future directions,” Front. Batter. Electrochem., vol. 5, p. 1764210, Jan. 2026, doi: 10.3389/fbael.2026.1764210.
11. S. Ramshankar and M. Manimozhi, “Integration of digital twin technologies for state estimation in electric vehicle batteries: A review,” Results in Engineering, vol. 27, p. 106858, Sep. 2025, doi: 10.1016/j.rineng.2025.106858.
12. B. Huang, W. Yu, M. Ma, X. Wei, and G. Wang, “Artificial-Intelligence-Based Energy Management Strategies for Hybrid Electric Vehicles: A Comprehensive Review,” Energies, vol. 18, no. 14, p. 3600, Jul. 2025, doi: 10.3390/en18143600.
13. X. Teng, Z. Shen, and Y. Zhang, “Rule-based symbolic AI computing-driven digital twin model for ex-ante energy evaluation of task-ambience air conditioning systems in zero-energy buildings,” Sustainable Cities and Society, vol. 134, p. 106947, Nov. 2025, doi: 10.1016/j.scs.2025.106947.
14. A. Skuza, E. M. Szumska, R. Jurecki, and A. Pawelec, “Modeling the Impact of Traffic Parameters on Electric Vehicle Energy Consumption,” Energies, vol. 17, no. 21, p. 5423, Oct. 2024, doi: 10.3390/en17215423.
15. N. Zhao, N. Schofield, R. Yang, and R. Gu, “Investigation of DC-Link Voltage and Temperature Variations on EV Traction System Design,” IEEE Trans. on Ind. Applicat., vol. 53, no. 4, pp. 3707–3718, Jul. 2017, doi: 10.1109/TIA.2017.2692198.
16. I. Saba, A. H. Alobaidi, S. Alghamdi, and M. Tariq, “Digital Twin and TD3-Enabled Optimization of xEV Energy Management in Vehicle-to-Grid Networks,” IEEE Access, vol. 13, pp. 92495–92506, 2025, doi: 10.1109/ACCESS.2025.3572345.
17. Y. Ye, B. Xu, H. Wang, J. Zhang, B. Lawler, and B. Ayalew, “Deep reinforcement learning-based energy management system enhancement using digital twin for electric vehicles,” Energy, vol. 312, p. 133384, Dec. 2024, doi: 10.1016/j.energy.2024.133384.
18. A. Castellano, P. Stano, U. Montanaro, M. Cammalleri, and A. Sorniotti, “Model predictive control for multimode power-split hybrid electric vehicles: Parametric internal model with integrated mode switch and variable meshing losses,” Mechanism and Machine Theory, vol. 192, p. 105543, Feb. 2024, doi: 10.1016/j.mechmachtheory.2023.105543.
19. Z. Chen, H. Hu, Y. Wu, Y. Zhang, G. Li, and Y. Liu, “Stochastic model predictive control for energy management of power-split plug-in hybrid electric vehicles based on reinforcement learning,” Energy, vol. 211, p. 118931, Nov. 2020, doi: 10.1016/j.energy.2020.118931.
20. P. Dong et al., “Practical application of energy management strategy for hybrid electric vehicles based on intelligent and connected technologies: Development stages, challenges, and future trends,” Renewable and Sustainable Energy Reviews, vol. 170, p. 112947, Dec. 2022, doi: 10.1016/j.rser.2022.112947.
21. H. A. Borhan, C. Zhang, A. Vahidi, A. M. Phillips, M. L. Kuang, and S. Di Cairano, “Nonlinear Model Predictive Control for power-split Hybrid Electric Vehicles,” in 49th IEEE Conference on Decision and Control (CDC), Atlanta, GA, USA: IEEE, Dec. 2010, pp. 4890–4895. doi: 10.1109/CDC.2010.5718075.
22. C.-T. Li, “DESIGN OF POWER-SPLIT HYBRID VEHICLES WITH A SINGLE PLANETARY GEAR.” 2012. [Online]. Available: https://huei.engin.umich.edu/wp-content/uploads/sites/186/2015/02/DSCC-2012-Zhang.pdf
23. MathWorks, “Build Hybrid Electric Vehicle Input Power-Split Model,” 2026, [Online]. Available: https://www.mathworks.com/help/autoblks/ug/explore-the-hybrid-electric-vehicle-input-power-split-reference-application.html
24. A. O. Polat, B. C. Erden, S. Kul, and F. Nasiroglu, “Light Electric Vehicle Performance with Digital Twin Technology: A Comparison of Motor Types,” Arab J Sci Eng, vol. 49, no. 5, pp. 7209–7222, May 2024, doi: 10.1007/s13369-023-08668-x.
25. H. Liu, “Active damping of driveline vibration in power-split hybrid vehicles based on model reference control,” 2019, [Online]. Available: https://pure.bit.edu.cn/en/publications/active-damping-of-driveline-vibration-in-power-split-hybrid-vehic/
26. C. Li, J. Lei, L. Yang, W. Xu, and Y. You, “Research on Electric Vehicle Powertrain Systems Based on Digital Twin Technology,” Electronics, vol. 13, no. 20, p. 4103, Oct. 2024, doi: 10.3390/electronics13204103.
27. M. Waseem, G. S. Lakshmi, E. Sreeshobha, and S. Khan, “An electric vehicle battery and management techniques: comprehensive review of important obstacles, new advancements, and recommendations,” Energy Storage and Saving, vol. 4, no. 1, pp. 83–108, Mar. 2025, doi: 10.1016/j.enss.2024.09.002.
28. K. S. S. Alamin, Y. Chen, E. Macii, M. Poncino, and S. Vinco, “A Machine Learning-based Digital Twin for Electric Vehicle Battery Modeling,” Jun. 16, 2022, arXiv: arXiv:2206.08080. doi: 10.48550/arXiv.2206.08080.
29. J. Van Mierlo, Plug-in Hybrid Electric Vehicle (PHEV). Erscheinungsort nicht ermittelbar: MDPI - Multidisciplinary Digital Publishing Institute, 2019.
30. N. Fachada, V. V. Lopes, R. C. Martins, and A. C. Rosa, “Model-independent comparison of simulation output,” Simulation Modelling Practice and Theory, vol. 72, pp. 131–149, Mar. 2017, doi: 10.1016/j.simpat.2016.12.013.
31. M. S. Es-haghi, C. Anitescu, and T. Rabczuk, “Methods for enabling real-time analysis in digital twins: A literature review,” Computers & Structures, vol. 297, p. 107342, Jul. 2024, doi: 10.1016/j.compstruc.2024.107342.
32. C. Wang et al., “A modeling method of digital twin connection model based on virtual sensor,” J Intell Manuf, vol. 37, no. 5, pp. 2183–2201, May 2026, doi: 10.1007/s10845-025-02639-9.